Available online at www.sciencedirect.com
SCIENCE DIRECT®
Biochemical Pharmacology 66 (2003) 1717–1726
Biochemical Pharmacology
www.elsevier.com/locate/biochempharm

Spin trapping of superoxide, alkyl- and lipid-derived radicals with derivatives of the spin trap EPPN

Klaus Stolze[a], Natascha Udilova[a], Thomas Rosenau[b], Andreas Hofinger[b], Hans Nohl[a,*]

[a]*Basic Pharmacology and Toxicology, Institute of Applied Botany, University of Veterinary Medicine Vienna, Veterinärplatz 1, A-1210 Vienna, Austria*
[b]*Institute of Chemistry, University of Agricultural Sciences, Muthgasse 18, A-1190 Vienna, Austria*

Received 10 February 2003; accepted 28 June 2003

Abstract

The *N*-*t*-butyl-α-phenylnitrone derivative *N*-2-(2-ethoxycarbonyl-propyl)-α-phenylnitrone (EPPN) has recently been reported to form a superoxide spin adduct ($t_{1/2} = 5.25$ min at pH 7.0), which is considerably more stable than the respective *N*-*t*-butyl-α-phenylnitrone or 5,5-dimethylpyrroline *N*-oxide adducts ($t_{1/2} \sim 10$ and 45 s, respectively). In continuation of our previous studies on structure optimization of 5-(ethoxycarbonyl)-5-methyl-1-pyrroline *N*-oxide derivatives, a series of six different EPPN derivatives was synthesized and characterized by ^{1}H NMR, ^{13}C NMR and IR spectroscopy. The ethoxy group of EPPN was replaced by a propoxy, *iso*-propoxy, *n*-butoxy, *sec*-butoxy, and *tert*-butoxy moiety, as well as the phenyl by a pyridyl ring. Electron spin resonance spectra and stabilities of the superoxide adducts of the propoxy derivatives were found to be similar to those of the respective EPPN adduct, whereas the electron spin resonance spectra of the superoxide adducts of *N*-2-(2-ethoxycarbonyl-propyl)-α-(4-pyridyl) nitrone and the butoxy derivatives were accompanied by decomposition products. In contrast to the 5-(ethoxycarbonyl)-5-methyl-1-pyrroline *N*-oxide series, no significant improvement of the superoxide adduct stability could be obtained when the ethoxy group was replaced by other substituents. Carbon centered radical adducts derived from methanol, ethanol, formic acid and linoleic acid hydroperoxide were more stable than those of 5,5-dimethylpyrroline *N*-oxide, whereas among the alkoxyl radicals only the methoxyl radical adduct could be detected.

Keywords: Spin traps; ESR; EPPN derivatives; Superoxide; Linoleic acid hydroperoxide; Free radicals

1. Introduction

The synthesis of the spin trap EPPN from benzaldoxime and ethyl 2-bromo-2-methylpropionate has recently been described by Roubaud *et al*. [1]. In contrast to the structurally related spin traps *N*-*t*-butyl-α-phenylnitrone (PBN) or α-(4-pyridyl-1-oxide)-*N*-*t*-butylnitrone (POBN), the superoxide spin adducts of which are practically undetectable due to their instability [2], the EPPN superoxide spin adduct has a half-life of about 5 min at pH 7 [1]. This value is comparable to the recently reported data of the spin traps 5-(ethoxycarbonyl)-5-methyl-1-pyrroline *N*-oxide (EMPO) ($t_{1/2} = 8.6$ min) [3–5] or 1,3,3-trimethyl-6-azabicyclo [3.2.1]oct-6-ene-*N*-oxide (Trazon, $t_{1/2} = 3.6$ min) [6,7], even though lower than the respective value of 5-(diethoxyphosphoryl)-5-methyl-1-pyrroline *N*-oxide (DEPMPO) ($t_{1/2} = 14.8$ min) [8,9]. Recent studies with EMPO derivatives demonstrated that the stability of the superoxide adducts was significantly increased when the ethoxy group was replaced by bulky substituents such as a *sec*-butyl or *tert*-butyl group [10]. Furthermore, due to their higher lipophilicity, these compounds were expected to be suitable for the investigation of radicals in lipid

* Corresponding author. Tel.: +43-1-25077-4400; fax: +43-1-25077-4490.
E-mail address: Hans.Nohl@vu-wien.ac.at (H. Nohl).

Abbreviations: BPPN, *N*-2-(2-butoxycarbonyl-propyl)-α-phenylnitrone; DEPMPO, 5-(diethoxyphosphoryl)-5-methyl-1-pyrroline *N*-oxide; DMPO, 5,5-dimethylpyrroline *N*-oxide; DTPA, diethylenetriaminepentaacetic acid; EMPO, 5-(ethoxycarbonyl)-5-methyl-1-pyrroline *N*-oxide; EPPN, *N*-2-(2-ethoxycarbonyl-propyl)-α-phenylnitrone; EPPyN, *N*-2-(2-ethoxycarbonyl-propyl)-α-(4-pyridyl) nitrone; ESR, electron spin resonance; HFS, hyperfine splitting; LO•, lipoxyl radical; NMR, nuclear magnetic resonance; $O_2^{\bullet -}$, superoxide anion radical; PBN, *N*-*t*-butyl-α-phenylnitrone; POBN, α-(4-pyridyl-1-oxide)-*N*-*t*-butylnitrone; PPPN, *N*-2-(2-propoxycarbonyl-propyl)-α-phenylnitrone; SOD, superoxide dismutase; Trazon, 1,3,3-trimethyl-6-azabicyclo [3.2.1]oct-6-ene-*N*-oxide.

0006-2952/$ – see front matter © 2003 Elsevier Inc. All rights reserved.
doi:10.1016/S0006-2952(03)00479-9

membranes. As a possible application, the detection of lipid peroxidation-derived free radicals has recently been investigated using different spin traps, such as 5,5-dimethyl-pyrroline *N*-oxide (DMPO) [11], DEPMPO [9,12], EMPO [5] or Trazon [7].

It was the aim of the present study to evaluate the effect of substituent modification in the ester moiety of EPPN on the stability of the radical adducts, especially with respect to the stability of oxygen centered radicals such as superoxide, hydroxyl or alkoxyl radicals. For this purpose, a modified synthetic approach was developed in accordance with a recently published synthetic procedure for the synthesis of the spin trap EMPO [3–5].

2. Materials and methods

2.1. Chemicals

2-Bromo-2-methylpropionyl bromide, linoleic acid, superoxide dismutase (SOD) and xanthine oxidase were commercially available from Sigma-Aldrich. Petroleum ether (high boiling, 50–70°) was obtained from Fluka, all other chemicals from Merck.

2.2. Syntheses

Synthesis and characterization of the compounds were performed according to the synthesis of EMPO and its derivatives [3–5] with minor adaptations.

2.2.1. Alkyl 2-bromo-2-methylpropionate

2-Bromo-2-methylpropionyl bromide (70 mmol) was slowly added to a solution of the respective alcohol (100 mmol) and pyridine (70 mmol) in chloroform at 0° (ice bath). After stirring for 1 hr, the reaction mixture was successively washed with water (50 mL), sulfuric acid (10%, 50 mL) and concentrated aqueous sodium bicarbonate (50 mL), and dried over Na_2SO_4 overnight. Solvent and excess alcohol were removed under reduced pressure. The crude, almost colorless product was used without further purification.

2.2.2. Alkyl 2-methyl-2-nitropropionate

The respective alkyl 2-bromo-2-methylpropionate (60 mmol) was added under stirring to a solution of sodium nitrite (7.2 g, 104 mmol) and phloroglucinol dihydrate (8.5 g, 52 mmol) in dry dimethylformamide (120 mL) at room temperature. The solution was stirred for 3 days, poured into ice water (240 mL) and extracted four times with ethyl acetate (100 mL). The combined extracts were treated twice with 100 mL of saturated sodium bicarbonate solution and dried over Na_2SO_4. After removal of the solids by filtration, the solvent was evaporated *in vacuo*. The obtained colorless or pale yellow products were used without further purification.

2.2.3. Synthesis of the N-oxides

To a concentrated solution of the respective alkyl 2-methyl-2-nitropropionate (25 mmol) in H_2O/CH_3OH (v/v = 6:4), benzaldehyde or pyridine-4-aldehyde (30 mmol) and aqueous ammonium chloride solution (1.87 g in 8 mL water) were added. The mixture was carefully kept at room temperature, while 3.27 g (50 mmol) zinc dust was slowly added within 30 min. After stirring for 4.5 hr at room temperature, the white precipitate and the remaining zinc powder was removed by filtration and the solid residue was washed five times with 30 mL of methanol. The combined liquid phases were concentrated to a volume of about 10 mL, saturated with borax and extracted four times with 60 mL of dichloromethane. The combined extracts were dried over sodium sulfate, filtered and concentrated. Column chromatography on silica gel (petroleum ether/ethanol (1–5%) with gradient elution) yielded approximately 20–30% of a light-brown product, which was recrystallized from pentane and characterized by ^{1}H NMR, ^{13}C NMR, and IR spectroscopy. The purity of the products was assessed by HPLC and UV spectroscopy.

2.2.4. Preparation of lipid hydroperoxides

Linoleic acid hydroperoxide was synthesized according to O'Brien [13]. Briefly, linoleic acid was air-oxidized for 72 hr in the dark at room temperature. The oxidation mixture was dissolved in petroleum ether (boiling range 60–90°) and extracted four times with water/methanol (v/v = 1:3). The obtained methanolic phase was counter-extracted four times with petroleum ether (boiling range 60–90°) and evaporated under reduced pressure. The obtained hydroperoxide was dissolved in ethanol and stored in liquid nitrogen. The concentration of hydroperoxide was determined based on an extinction coefficient of $\varepsilon_{233\,nm} = 25{,}250\ M^{-1}\ cm^{-1}$ in ethanol [13].

2.3. Instruments

UV-Vis spectra were recorded on Hitachi 150-20 and U-3300 spectrophotometers in the double beam mode against a reference sample of the respective solvent. Determination of the concentrations was done measuring the absorption maxima in the range between 200 and 350 nm.

IR spectra were recorded as film spectra on a ATI Mattson Genesis Series FTIR spectrometer.

For electron spin resonance (ESR) experiments the Bruker spectrometers ER 200 D-SRC 9/2.7 with the data system ESP1600 and the ESP300E were used, operating at 9.6 GHz with 100 kHz modulation frequency, equipped with a rectangular TE_{102} or a TM_{110} microwave cavity.

^{1}H NMR spectra were recorded at 300 MHz, ^{13}C NMR spectra at 75.47 MHz on a Bruker Avance. $CDCl_3$ containing tetramethylsilane (TMS) as the internal standard was used as the solvent throughout. ^{13}C peaks were assigned by means of APT (attached proton test), HMQC (^{1}H-detected heteronuclear multiple-quantum coherence) and HMBC

(heteronuclear multiple bond connectivity) spectra. A complete set of ^{1}H, H–H correlated, ^{13}C, HMQC and HMBC spectra was recorded for each compound. All chemical shift data are given in ppm units.

Computations, as implemented through Spartan Pro 02 by Wavefunction, Inc., Irvine, CA, USA, were carried out on the superoxide spin adducts of EPPN, *N*-2-(2-butoxycarbonyl-propyl)-α-phenylnitrone (BPPN) and *t*BPPN.[1] Starting geometries were obtained by conformational search, followed by pre-optimization of the minimum conformers by the semi-empirical PM3 method. For full geometry optimization of each structure, the widely employed hybrid method denoted by B3LYP [14], which includes a mixture of HF and DFT exchange terms and the gradient-corrected correlation functional of Lee *et al.* [15,16], as proposed and parametrized by Becke [17,18], was used, along with the double-zeta split valence basis sets 6-31 + G* [19], which includes diffuse functions.

3. Results

The identity of the synthesized spin traps was unambiguously proven by NMR. In the ^{1}H NMR spectra, the benzylidenic proton appeared throughout as a singlet without long-range couplings, usually at 7.49 ppm. The signal with the highest down-field shift originates from the magnetically equivalent protons at C-2 and C-6 of the phenyl ring. The resonances of the protons at C-3, C-5 and C-4 of the phenyl ring generally overlapped, in some derivatives also with the benzylidenic proton. The inductive effect of secondary and tertiary alkoxy substituents in the ester group was noticeable, but caused a small up-field shift (0.03–0.07 ppm) only.

The four ^{13}C NMR resonances (C-1, C-2/6, C-3/5, C-4) of the phenyl substituent appeared at averaged values of 130.4, 129.0, 128.5 and 130.6 ppm, respectively. The carbonyl propyl moiety gave signals at 24.5 ppm (methyl), 77.1 ppm (quaternary carbon) and 170 ppm (carboxyl group). The ^{13}C NMR data were very consistent, without significant influences of the ester moieties on the resonances of the nitrone being noticeable. In N–O derivatives with a C=N double bond, such as oximes, nitroxides or nitrones, the *Z*-configured α-C atoms are characteristically shifted upfield by 6–10 ppm [20]. With an expected resonance at about 135–140 ppm, the chemical shift of the benzylidenic carbon at 130 ppm is indicative of its *Z*-arrangement with regard to the oxygen. Thus, only the isomers with the C=N double bond in *E*-configuration were formed in the synthesis, so that the sterically demanding substituents, i.e. the phenyl ring and the alkylester moiety, are placed *trans*. The respective NMR and IR data are summarized in Tables 1–3.

[1] The complete computational output can be obtained from the authors upon request. Computational data of the spin trap starting materials are available as well.

3.1. Spin trapping of superoxide radicals

Figure 1 shows the general structure of the spin traps used. Figure 2a represents the ESR spectrum of the superoxide adduct of EPPN (20 mM) generated in the xanthine/xanthine oxidase system at pH 5.8, the optimal value for its detection [1]. Five percent DMSO was included to allow comparison with the less water-soluble derivatives *N*-2-(2-propoxycarbonyl-propyl)-α-phenylnitrone (PPPN) (Fig. 2b) and *i*PPPN (Fig. 2c), from which ESR spectra of similar resolution and intensity could be obtained. From the highly lipophilic derivatives BPPN, *s*BPPN, and *t*BPPN only composite ESR spectra could be obtained, with a high contribution of degradation products, most probably the bis(2-alkoxycarbonyl-propyl) nitroxide, giving a triplet comparable to di-*tert*-butyl nitroxide (spectrum not shown). The ESR spectrum obtained from the *N*-2-(2-ethoxycarbonyl-propyl)-α-(4-pyridyl) nitrone (EPPyN) superoxide adduct (a_N = 13.67 G; a_H = 1.60 G) was accompanied by the six line spectrum of an unknown degradation product (a_N = 15.25 G; a_H = 2.6 G). The spectral parameters of the latter compounds (see Table 5) had therefore to be calculated from the difference spectra obtained by subtraction of the secondary product spectra. For this reason, hyperfine splitting (HFS) values and half-life of the superoxide adducts of EPPyN, BPPN, *s*BPPN, and *t*BPPN could only be approximated (Tables 4 and 5). For the determination of $t_{1/2}$ of the superoxide adducts the best results were obtained when the respective spin traps (20 mM, final concentration) were incubated in water/DMSO in the presence of approximately 0.5 mg solid KO_2 for 15 s, after which phosphate buffer (300 mM, final pH 7.0, containing 20 mM DTPA, SOD (100 U/mL), catalase (250 U/mL) and 5% DMSO) was added. Several consecutive spectra were recorded until the superoxide-related lines disappeared. Several accompanying lines of low intensity, probably from a carbon-centered degradation product, were subtracted from the individual ESR spectra before calculating the $t_{1/2}$ values from the corrected intensity decrease of the first two lines as a first order exponential fit. The respective values are listed in Table 4.

The low stability of the superoxide adducts as compared to those of the EMPO series can be correlated with the molecular structure as obtained from DFT computations. For EMPO derivatives it was found that the stability of the superoxide adducts was largely governed by the steric environment of the nitroxyl group, with bulky alkoxy substituents shielding the nitroxyl group, thus increasing the stability of the superoxide adducts, while the spin density distribution was nearly identical for all EMPO derivatives [10]. As in the case of EMPO derivatives, also in EPPN derivatives the spin density distribution was not influenced by alteration of the alkoxy substituent. However, while in the EMPO series the alkoxy substituents are always held in close proximity to the nitroxyl group due to

Table 1
^{13}C NMR data (ppm) of the spin traps

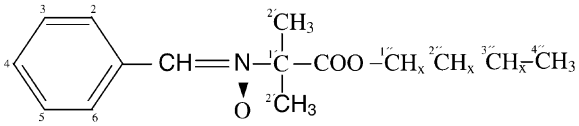

	^{1}C	^{2,6}C	^{3,5}C	^{4}C	CH	$^{1'}$C	$^{2'}$C	COO	$^{1''}$C	$^{2''}$C	$^{3''}$C	$^{4''}$C
EPPN	130.4	129.1	128.6	130.7	131.3	77.1	24.5	170.6	62.1	14.0	–	–
PPPN	130.4	129.0	128.5	130.6	131.2	77.1	24.5	170.6	67.6	21.8	10.3	–
*i*PPPN	130.56	129.0	128.5	130.54	131.2	77.1	24.5	170.1	69.8	21.5	–	–
BPPN	130.4	129.0	128.5	130.6	131.2	77.2	24.5	170.6	65.9	30.4	19.0	13.7
*s*BPPN	130.52	128.9	128.5	130.47	131.1	77.2	24.4	170.2	74.2$^{(2'')}$	19.2$^{(1'')}$	28.6	9.6
*t*BPPN	130.7	129.0	128.6	130.5	131.1	77.2	24.6	169.8	82.5	27.8	–	–
EPPyN	137.3[a]	121.8[a]	149.7[a]	–	129.0[a]	78.3[a]	24.4[a]	169.9[a]	62.3[a]	13.9[a]		

[a] Positions in analogy to EPPN.

the geometry requirements of the heterocyclic ring system, the aliphatic chain structure of EPPN derivatives renders these compounds much more flexible. Thus, the alkoxy substituent in the ester group loses its influence as the spatial distance to the spin-bearing nitroxyl group is much larger. DFT computations confirmed that the distance between the nitrogen and carbon C-1 of the alkoxy group in superoxide adducts of EMPO derivatives ranged around 4.2 Å, whereas that in EPPN derivatives is approximately 0.5 Å larger. The same applies to the distance between the nitroxyl oxygen and C-1, which is on average 4.3 Å in EMPO superoxide spin adducts, but 4.8 Å in those of EPPN. The low steric shielding of the nitroxyl group by the alkoxycarbonyl moiety in the spin adducts of EPPN derivatives must thus be assumed to be the major cause of their observed lower stability.

3.2. Spin adduct formation with oxygen-containing radicals

Spin adduct formation in the presence of any EPPN derivative with hydroxyl radicals using a Fenton system did not result in the detection of the respective hydroxyl adducts. Instead, a carbon-centered radical adduct was formed in the case of incubation times less than 30 s (Table 5, spectrum not shown). After prolonged incubation, the respective (2-alkoxycarbonyl-propyl)-2-aminoxyl [1] was observed as the predominant species (shown below, Fig. 4b).

In the presence of methanol and iron, two different radical adducts could be detected. A Fenton system in the presence of 5% methanol according to Roubaud *et al.* [1] resulted in the formation of the respective hydroxymethyl radical adduct, as shown in Fig. 3a for the EPPN/$^{\bullet}CH_2OH$ species. In Fig. 3b the ESR spectrum of the methoxyl radical adduct of EPPN is shown (marked "x"), which was obtained after nucleophilic addition of methanol to EPPN in the presence of Fe^{3+} using experimental conditions reported by Dikalov and Mason [11], except that the incubation time was reduced to 10 s in order to suppress the formation of the (2-ethoxycarbonyl-propyl)-2-aminoxyl radical (marked "o").

The observed HFS values ($a_N = 14.56$ G; $a_H = 4.16$ G) are clearly different from the hydroxymethyl radical

Table 2
^{1}H NMR data (ppm) of the spin traps

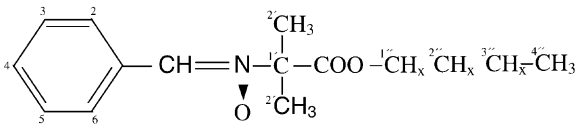

	^{2,6}CH	^{3,5}CH	^{4}CH	HC=N	$^{2'}$CH$_3$	OCH$_x$	$^{2''}$CH$_x$	$^{3''}$CH$_x$	$^{4''}$CH$_3$
EPPN	8.28m	7.42m	7.42m	7.49s	1.82s	4.25q	1.27t	–	–
PPPN	8.28m	7.42m	7.42m	7.49s	1.82s	4.19t	1.66m	0.91t	–
*i*PPPN	8.27m	7.41m	7.41m	7.45s	1.80s	5.10sp	1.25d	–	–
BPPN	8.27m	7.42m	7.42m	7.49s	1.82s	4.20t	1.63qi	1.35m	0.89t
*s*BPPN	8.27m	7.41m	7.41m	7.46s	1.81s	4.93sx$^{(2'')}$	1.22d$^{(1'')}$	1.59m	0.87t
*t*BPPN	8.25m	7.42m	7.42m	7.42s	1.77s	–	1.48s	–	–
EPPyN[a]	8.09d[a]	8.69d[a]	–	7.55s[a]	1.84s[a]	4.26q[a]	1.28t[a]		

[a] Positions in analogy to EPPN.

Table 3
IR data (cm^{-1}) of the spin traps

EPPN	3091	3058	2985	2939	**1742**	**1580**	1563	**1469**	**1446**	**1413**	**1387**	**1364**	**1280**	**1177**	**1154**	**1119**	–	**1025**	–	906	–	859	808	755	**693**
PPPN	3080	3057	2966	2939	**1743**	1581	1563	1469	**1447**	1414	1390	1364	**1283**	**1162**	–	**1112**	–	1054	963	900	–	856	813	756	**693**
*i*PPPN	3079	3063	2983	2938	**1742**	1582	1567	1468	**1447**	1418	1386	**1374**	**1278**	**1169**	–	**1112**	**1101**	–	957	898	–	839	817	754	692
BPPN	3090	3057	**2959**	2936	**1745**	1579	1555	1467	**1446**	1413	1390	1364	**1281**	**1164**	–	**1121**	–	1020	–	900	–	–	805	754	**693**
*s*BPPN	3085	3058	**2973**	2938	**1740**	1581	1564	1468	**1447**	1415	1385	1365	**1280**	**1169**	–	**1113**	1090	1028	969	909	882	866	805	753	**693**
*t*BPPN	3078	3053	**2984**	**2928**	**1738**	**1581**	1566	**1468**	**1445**	1416	**1386**	**1364**	**1288**	**1144**	–	**1112**	–	954/927		904	–	**844**	–	**752**	**690**
EPPyN	3085	3035	2983	2939	**1742**	**1593**	**1571**	1469	1445	**1416**	1389	**1365**	**1281**	**1177**	**1156**	**1133**	–	1024	989	910	–	**839**	794	762	695
PBN	3092	3054	**2975**	2934	–	1577	**1557**	1479	**1445**	**1409**	**1362**	–	–	**1193**	–	**1125**	–	–	–	907	–	802	–	752	**693**
POBN	3119	3035	2982	2946	–	–	**1555**	1466	**1436**	**1409**	**1361**	–	**1265**	**1239**	–	**1124**	1095	–	–	912	–	**841**	–	–	–

Intensities: strong (**1742**), medium (**1580**), weak (1563).

EPPN: R = C_2H_5
PPPN: R = C_3H_7
iPPPN: R = iso-C_3H_7
BPPN: R = n-C_4H_9
sBPPN: R = sec-C_4H_9
tBPPN: R = tert-C_4H_9

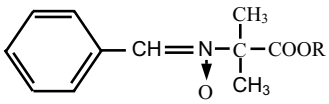

EPPyN:

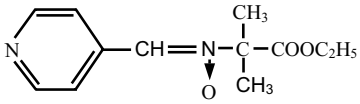

Fig. 1. General structure of the spin traps.

adduct obtained in the above mentioned Fenton system containing 5% methanol (a_N = 15.29 G; a_H = 3.80 G).

When ^{13}C-labeled methanol was used, an additional splitting was observed in the case of the carbon-centered hydroxymethyl radical adduct (e.g. for EPPN/$^{\bullet}CH_2OH$: $a_{^{13}C}$ = 3.60 G), whereas the spectrum of the oxygen centered methoxyl radical adduct (EPPN/$^{\bullet}OCH_3$) remained unchanged (Table 5, spectra not shown).

With other alcohols only the respective hydroxyalkyl radical adducts were observed, e.g. the EPPN/$^{\bullet}C(CH_3)_2(OH)$ adduct shown in Fig. 4a, obtained in a Fenton system containing 5% 2-propanol. No 2-propoxyl radical adduct of EPPN was obtained after nucleophilic addition of 2-propanol to EPPN in the presence of Fe^{3+} using the same conditions as with methanol. Instead, a four-line ESR spectrum from a decomposition product appeared (Fig. 4b), which can be assigned to the (2-ethoxycarbonyl-propyl)-2-aminoxyl (a_N = 13.5 G; a_H = 13.4 G) [1].

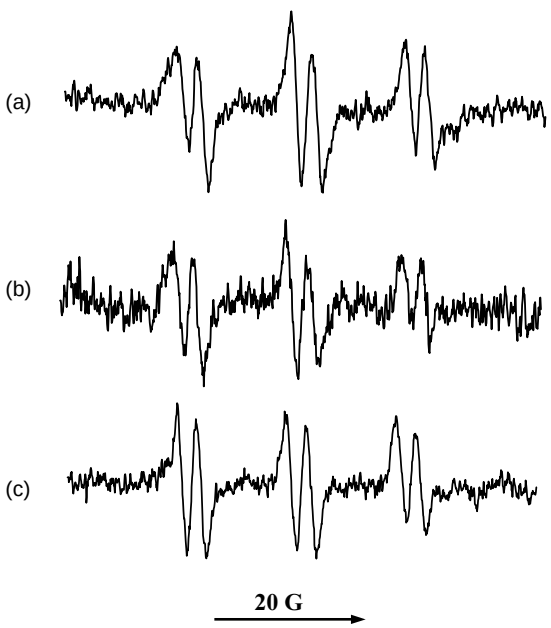

Fig. 2. Formation of the superoxide adducts of the spin traps EPPN, PPPN and *i*PPPN using the xanthine/xanthine oxidase system. (a) EPPN (20 mM), catalase (250 U/mL), xanthine (0.2 mM) and xanthine oxidase (50 mU/mL) in oxygenated phosphate buffered saline (20 mM, pH 5.8, containing 0.4 mM DTPA and 5% DMSO) were aspirated into the flat cell using the rapid sampling technique and measured using the following ESR parameters: sweep width, 60 G; modulation amplitude, 1.50 G; microwave power, 50 mW; time constant, 0.16 s; receiver gain, 2×10^5; scan rate, 43.9 G/min. (b) Same as in (a), except that PPPN (20 mM) was used. (c) Same as in (a), except that *i*PPPN (20 mM) was used.

3.3. Spin trapping of lipid-derived free radicals

For the detection of lipid-derived free radicals two different radical generating systems were selected. The first system was anaerobic (flushed with nitrogen for several minutes) and consisted of peroxidized linoleic acid and the spin trap dissolved in 20 mM phosphate buffer, pH 7.4, containing 1.5% acetonitrile. To this solution Fe^{2+}, dissolved in nitrogen-purged water, was added in order to start the formation of free radicals in a Fenton-type reaction, as recently tested with different DEPMPO derivatives in both aerobic and anaerobic environment [3,4] using a stationary system in combination with the rapid sampling technique.

In Fig. 5a, the EPPN adduct of the radical derived from linoleic acid hydroperoxide generated in the anaerobic Fenton is shown, its spectral parameters as obtained by computer simulation (Fig. 5b) being typical of a partially immobilized carbon centered radical adduct (see also Table 5). No additional radical adducts could be detected even when the concentration of EPPN was increased to

Table 4
Half-lives of the superoxide adducts and *n*-octanol/water partition coefficients of the spin traps

Acronym	Apparent $t_{1/2}$ (min)	Partition coefficient *n*-octanol/phosphate buffer (100 mM, pH 7.4)
EPPN	5.90	29.8[a]
PPPN	3.45	57
*i*PPPN	5.37	60
BPPN	<1	219
*s*BPPN	2.51	207
*t*BPPN	~1[b]	145
EPPyN	7.28	3.7

[a] Data from Roubaud *et al.* [1].
[b] Approximated value due to formation of decomposition products.

Table 5
Comparison of the ESR parameters of different radical adducts of various EPPN derivatives

Radical HFS (G)		EPPN	PPPN	*i*PPPN	BPPN	*s*BPPN	*t*BPPN	EPPyN
•OOH	a_N	14.18	14.2	14.10	14.2	14.12	14.1	13.67
	a_H	2.47	2.5	2.49	2.5	2.48	2.5	1.60
•C (“•OH”)	a_N	15.07	15.11	15.05	15.11	15.07	15.07	14.67
	a_H	4.88	4.93	4.88	4.87	4.77	4.72	3.43
•H	a_N	16.05	16.02	16.01	16.02	15.98	16.05	15.65
	a_H	10.50	10.46	10.64	10.46	10.64	10.80	9.99
•CH_3	a_N	15.72	15.71	15.67	15.67	15.65	15.69	14.66
	a_H	3.89	3.96	3.97	3.95	4.03	4.00	3.43
•OCH_3	a_N	14.56	14.55	14.54	14.50	14.47	14.53	14.05
	a_H	4.16	4.15	4.19	4.10	4.15	4.26	3.03
•CH_2OH	a_N	15.29	15.29	15.24	15.29	15.19	15.24	14.92
	a_H	3.80	3.87	3.85	3.80	3.95	4.02	3.09
	$a_{^{13}C}$	3.60	3.57	3.85	3.64	3.67	3.71	3.99
•$CH(OH)CH_3$	a_N	15.42	15.40	15.33	15.41	15.29	15.35	14.95
	a_H	3.20	3.23	3.25	3.26	3.33	3.42	2.65
•$C(CH_3)_2OH$	a_N	15.43	15.42	15.35	15.41	15.35	15.43	14.97
	a_H	3.47	3.47	3.57	3.40	3.60	3.64	2.63
•CO_2^-	a_N	15.19	15.16	15.14	15.13	15.10	15.16	14.95
	a_H	4.49	4.60	4.75	4.64	4.99	4.90	3.49
•OOL[a]	a_N	15.53	15.53	15.54	15.55	15.56	15.60	15.23
	a_H	2.42	2.40	2.42	2.28	2.40	2.42	2.67
•OOL[b]	a_N	15.44	15.53	15.55	15.59	15.43	15.57	15.26
	a_H	3.37	3.24	3.39	3.22	3.64	3.60	2.69

[a] LOOH/Fe^{3+}.
[b] LOOH/Fe^{2+}.

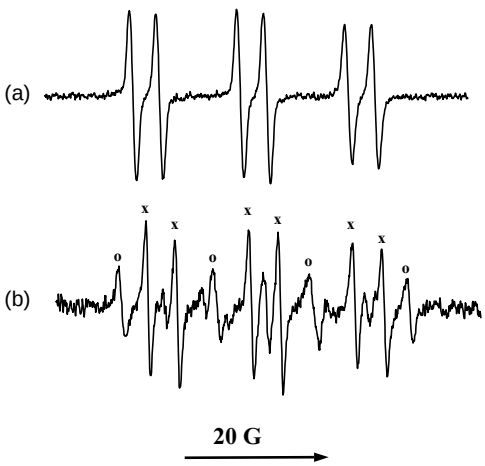

Fig. 3. Iron-dependent formation of two different EPPN spin adducts from methanol. (a) EPPN (10 mM) was incubated with a Fenton system containing 10% methanol, $FeSO_4$ (1 mM), EDTA (2 mM), H_2O_2 (0.2%) and the reaction was stopped after 10 s by 1:1 dilution with phosphate buffer (0.3 M, pH 7.4, containing 20 mM DTPA) and the solution immediately aspirated into the flat cell. The spectrum was recorded with the following spectrometer settings: sweep width, 60 G; modulation amplitude, 0.24 G; microwave power, 2 mW; time constant, 0.164 s; receiver gain, 2×10^5; scan rate, 21.5 G/min. (b) After a 10 s incubation of EPPN (100 mM in methanol) with $FeCl_3$ (10 mM), the reaction was stopped by 1:20 dilution with phosphate buffer (0.15 M, pH 7.4, containing 10 mM DTPA), and the solution aspirated into the flat cell using a rapid sampler. The spectrum was recorded with the following spectrometer settings: sweep width, 60 G; modulation amplitude, 0.67 G; microwave power, 20 mW; time constant, 0.02 s; receiver gain, 2×10^5; scan rate, 171.7 G/min.

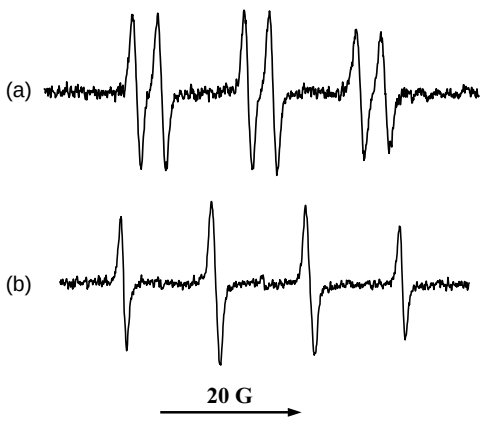

Fig. 4. Iron-dependent formation of two different EPPN spin adducts from 2-propanol. (a) EPPN (10 mM) was incubated with a Fenton system containing 10% 2-propanol, $FeSO_4$ (1 mM), EDTA (2 mM), H_2O_2 (0.2%) and the reaction was stopped after 10 s by 1:1 dilution with phosphate buffer (0.3 M, pH 7.4, containing 20 mM DTPA) and the solution immediately aspirated into the flat cell. The spectrum was recorded with the following spectrometer settings: sweep width, 60 G; modulation amplitude, 0.24 G; microwave power, 2 mW; time constant, 0.164 s; receiver gain, 2×10^5; scan rate, 21.5 G/min. (b) After a 10 s incubation of EPPN (100 mM in 2-propanol) with $FeCl_3$ (10 mM), the reaction was stopped by 1:20 dilution with phosphate buffer (0.15 M, pH 7.4, containing 10 mM DTPA), and the solution aspirated into the flat cell using a rapid sampler. The spectrum was recorded with the following spectrometer settings: sweep width, 60 G; modulation amplitude, 0.67 G; microwave power, 20 mW; time constant, 0.02 s; receiver gain, 2×10^5; scan rate, 171.7 G/min.

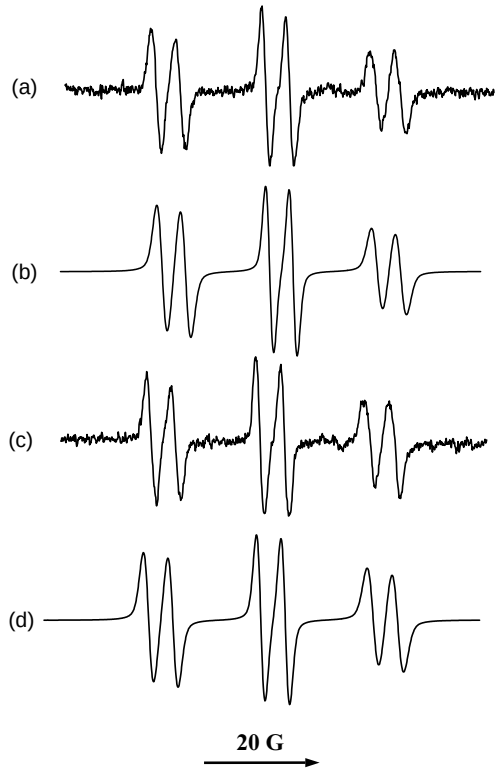

Fig. 5. Detection of a lipid-derived radical adduct from preoxidized linoleic acid using a Fenton-type incubation system in the presence of the spin traps EPPN and *i*PPPN. (a) To a nitrogen-bubbled solution of peroxidized linoleic acid (2.5 mM) and EPPN (20 mM) in phosphate buffer (20 mM, pH 7.4, containing 1.5% acetonitrile) $FeSO_4$ (0.1 mM) was added and the solution was aspirated under nitrogen into the flat cell using a rapid sampler. The spectrum was recorded with the following spectrometer settings: sweep width, 60 G; modulation amplitude, 1 G; microwave power, 2 mW; time constant, 0.08 s; receiver gain, 1×10^5; scan rate, 42.9 G/min. (b) Computer simulation using the following parameters: $a_N = 15.44$ G; $a_H = 3.37$ G; $\Delta H = 1.40$, 1.00, 1.55 G (1st, 2nd and 3rd doublet, respectively); 0.4 Lorentz/Gauss. (c) Same as in (a), except that *i*PPPN (20 mM) was used. (d) Computer simulation, using the following parameters: $a_N = 15.55$ G; $a_H = 3.39$ G; $\Delta H = 1.30$, 1.05, 1.55 G (1st, 2nd and 3rd doublet, respectively; 0.4 Lorentz/Gauss.

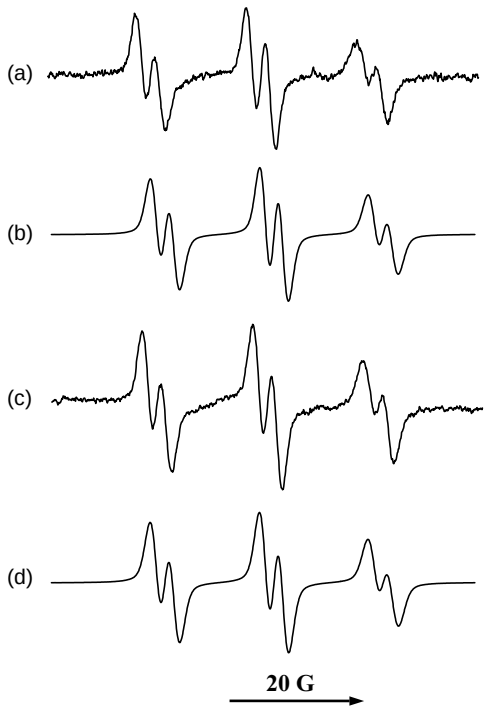

Fig. 6. Detection of lipid-derived radical adducts from preoxidized linoleic acid after Fe^{3+} catalyzed addition in the presence of the spin traps EPPN and *i*PPPN. (a) A mixture of peroxidized linoleic acid (5.5 mM), $FeCl_3$ (5 mM) and EPPN (20 mM), previously incubated for 5 min and then 1:30 diluted in with phosphate buffer (300 mM, pH 7.4, containing 20 mM DTPA), was aspirated using a rapid sampler and measured under the following conditions: sweep width, 60 G; modulation amplitude, 1.5 G; microwave power, 2 mW; time constant, 0.04 s; receiver gain, 1×10^5; scan rate, 171.7 G/min. (b) Computer simulation, using the following parameters: $a_N = 15.53$ G; $a_H = 2.42$ G; $\Delta H = 1.70$, 1.60, 1.85 G (1st, 2nd and 3rd doublet, respectively); 0.4 Lorentz/Gauss. (c) Same as in (a), except that *i*PPPN (10 mM) was used. (d) Computer simulation, using the following parameters: $a_N = 15.54$ G; $a_H = 2.42$ G; $\Delta H = 1.75$, 1.70, 1.95 G (1st, 2nd and 3rd doublet, respectively); 0.4 Lorentz/Gauss.

100 mM, which was possible in the presence of 20% acetonitrile or DMSO (spectra not shown).

Similarly, the respective *i*PPPN adduct was obtained (Fig. 5c) and characterized by computer simulation (Fig. 5d). As compared to the respective spin adducts with DMPO or DEPMPO, the adducts of the EPPN derivatives were considerably more stable (ca. 10–30 min).

The second system used aerobic incubation for 5 min in the presence of Fe^{3+} [11], followed by addition of the iron chelator DTPA in phosphate buffer.

The ESR spectrum obtained from EPPN and peroxidized linoleic acid is shown in Fig. 6a. The spectral parameters, obtained by computer simulation of the spectrum (Fig. 6b) can be interpreted in terms of a partially immobilized ESR spectrum different from the species obtained in the Fenton system. Although the nitrogen coupling constant suggests the formation of a carbon-centered radical, the value of the hydrogen splitting is exceptionally small. From *i*PPPN similar experimental (Fig. 6c) and simulated (Fig. 6d) spectra were obtained. The data of the other investigated spin traps are summarized in Table 5.

4. Discussion

Six novel EPPN derivatives were synthesized and characterized in this study. EPPN and its derivatives form only moderately stable superoxide adducts ($t_{1/2} = 1$–7 min), which are, however, more stable than the adducts with DMPO ($t_{1/2} = 45$ s [21]) or PBN [2]. In contrast, the superoxide adducts of some derivatives of EMPO ($t_{1/2} > 20$ min [10]) or DEPMPO ($t_{1/2} =\sim 7$–15 min [8,9,12]) are considerably more stable.

Although in our experiments no alkoxyl radical spin adducts could be detected, no definitive statement about their stability can be made. Alkoxyl radicals undergo rapid β-scission with a rate constant of around 10^6, which

efficiently competes with the spin trapping reaction, especially since higher concentrations of EPPN and its derivatives cannot be obtained, the maximum being about 50 mM in water and 100 mM in the presence of 20% acetonitrile or DMSO.

However, carbon centered radical adducts formed according to several pathways [22] in secondary reactions from $LOO^{\bullet}$ [23–28] and $LO^{\bullet}$ are very stable and could easily be detected. Although the structure of the various secondary radical adducts is not clear, the most likely positions of the oxygen on the peroxidized linoleic acid are the positions 9 and 13:

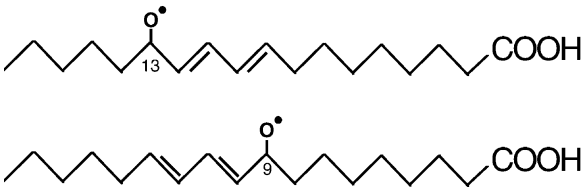

Depending on the reaction conditions (anaerobic, oxygenated, transition metal-catalyzed, etc.) a variety of carbon-centered radicals can be formed from these primary radicals, two of which have been shown in Figs. 5 and 6.

In conclusion, EPPN and its derivatives can be recommended for the detection of carbon-centered radicals, since the stability of their carbon-centered radical spin adducts seems to be comparable to those of PBN. In this respect, the investigated spin traps are possible alternatives to PBN, especially as a series of homologous spin traps with increasing lipophilicity can readily be synthesized from commercially available compounds in two or three steps. On the other hand, these novel spin traps do not seem to be suitable for the detection of oxygen-centered radicals, since their superoxide radical adducts are only moderately stable, and adducts with hydroxyl radicals could not be detected at all. Except for the moderately stable methoxyl adduct, no alkoxyl radical adducts were observed.

Acknowledgments

The authors wish to thank G. Marik and R. Stadtmüller for skillful technical assistance in synthesis, purification and characterization of the spin traps. The present investigation was supported by the Austrian Fonds zur Förderung der wissenschaftlichen Forschung.

References

[1] Roubaud V, Lauricella R, Bouteiller JC, Tuccio B. *N*-2-(2-Ethoxycarbonyl-propyl)-α-phenylnitrone: an efficacious lipophilic spin trap for superoxide detection. Arch Biochem Biophys 2002;397:51–6.

[2] Janzen EG, Kotake Y, Hinton RD. Stabilities of hydroxyl radical spin adducts of PBN-type spin traps. Free Radic Biol Med 1992;12:169–73.

[3] Olive G, Mercier A, LeMoigne F, Rockenbauer A, Tordo P. 2-Ethoxycarbonyl-2-methyl-3,4-dihydro-2*H*-pyrrole-1-oxide: evaluation of the spin trapping properties. Free Radic Biol Med 2000;28:403–8.

[4] Zhang H, Joseph J, Vasquez-Vivar J, Karoui H, Nsanzumuhire C, Martásek P, Tordo P, Kalyanaraman B. Detection of superoxide anion using an isotopically labeled nitrone spin trap: potential biological applications. FEBS Lett 2000;473:58–62.

[5] Stolze K, Udilova N, Nohl H. Spin adducts of superoxide, alkoxyl, and lipid-derived radicals with EMPO and its derivatives. Biol Chem 2002;383:813–20.

[6] Sankuratri N, Janzen EG. Synthesis and spin trapping chemistry of a novel bicyclic nitrone: 1,3,3-trimethyl-6-azabicyclo[3.2.1]oct-6-ene-*N*-oxide (Trazon). Tetrahedron Lett 1996;37:5313–6.

[7] Stolze K, Udilova N, Nohl H. ESR analysis of spin adducts of alkoxyl and lipid-derived radicals with the spin trap Trazon. Biochem Pharmacol 2002;63:1465–70.

[8] Fréjaville C, Karoui H, Tuccio B, Le Moigne F, Culcasi M, Pietri S, Lauricella R, Tordo P. 5-(Diethoxyphosphoryl)-5-methyl-1-pyrroline *N*-oxide: a new efficient phosphorylated nitrone for the in vitro and in vivo spin trapping of oxygen-centered radicals. J Med Chem 1995;38:258–65.

[9] Stolze K, Udilova N, Nohl H. Spin trapping of lipid radicals with DEPMPO-derived spin traps: detection of superoxide, alkyl and alkoxyl radicals in aqueous and lipid phase. Free Radic Biol Med 2000;29:1005–14.

[10] Stolze K, Udilova N, Rosenau T, Hofinger A, Nohl H. Synthesis and characterization of EMPO-derived 5,5-disubstituted 1-pyrroline *N*-oxides as spin traps forming exceptionally stable superoxide spin adducts. Biol Chem 2003;384:493–500.

[11] Dikalov SI, Mason RP. Spin trapping of polyunsaturated fatty acid-derived peroxyl radicals: reassignment to alkoxyl radical adducts. Free Radic Biol Med 2001;30:187–97.

[12] Stolze K, Udilova N, Nohl H. Lipid radicals: properties and detection by spin trapping. Acta Biochim Polon 2000;47:923–30.

[13] O'Brien PJ. Intracellular mechanisms for the decomposition of a lipid peroxide. I. Decomposition of a lipid peroxide by metal ions, heme compounds, and nucleophiles. Can J Biochem 1969;47:485–92.

[14] Russo TV, Martin RL, Hay PJ. Effective core potentials for DFT calculations. J Phys Chem 1995;99:17085–7.

[15] Lee C, Yang W, Parr RG. Development of the Colle-Salvetti correlation-energy formula into a functional of the electron density. Phys Rev B 1988;37(2):785–9.

[16] Miehlich B, Savin A, Stoll H, Preuss H. Results obtained with the correlation energy density functionals of Becke and Lee, Yang and Parr. Chem Phys Lett 1989;157(3):200–6.

[17] Becke A. Density-functional exchange-energy approximation with correct asymptotic behavior. Phys Rev A 1988;38(6):3098–100.

[18] Becke A. Density-functional thermochemistry. III. The role of exact exchange. J Chem Phys 1993;98(7):5648–52.

[19] Francl MM, Pietro WJ, Hehre WJ, Binkley JS, Gordon MS, DeFrees DJ, Pople JA. Self-consistent molecular orbital methods. XXIII. A polarization-type basis set for second-row elements. J Chem Phys 1982;77(7):3654–65.

[20] Hawkes GE, Herwig K, Roberts JD. Nuclear magnetic resonance spectroscopy, use of ^{13}C spectra to establish configurations of oximes. J Org Chem 1974;39:1017–28.

[21] Buettner GR, Oberley LW. Considerations in the spin trapping of superoxide and hydroxyl radical in aqueous systems using 5,5-dimethyl-1-pyrroline-1-oxide. Biochem Biophys Res Commun 1978;83:69–74.

[22] Rota C, Barr DP, Martin MV, Guengerich FP, Tomasi A, Mason RP. Detection of free radicals produced from the reaction of cytochrome P-450 with linoleic acid hydroperoxide. Biochem J 1997;328:565–71.

[23] Van der Zee J, Barr DP, Mason RP. ESR spin trapping investigation of radical formation from the reaction between hematin

and *tert*-butyl hydroperoxide. Free Radic Biol Med 1996;20: 199–206.

[24] Akaike T, Sato K, Ijiri S, Miyamoto Y, Kohno M, Ando M, Maeda H. Bactericidal activity of alkyl peroxyl radicals generated by heme-iron-catalyzed decomposition of organic peroxides. Arch Biochem Biophys 1992;294:55–63.

[25] Kalyanaraman B, Mottley C, Mason RP. A direct ESR and spin-trapping investigation of peroxyl free radical formation by hematin/hydroperoxide systems. J Biol Chem 1983;258:3855–8.

[26] Chamulitrat W, Takahashi N, Mason RP. Peroxyl, alkoxyl, and carbon-centered radical formation from organic hydroperoxides by chloroperoxidase. J Biol Chem 1989;264:7889–99.

[27] Davies MJ. Detection of peroxyl and alkoxyl radicals produced by reaction of hydroperoxides with heme-proteins by ESR spectroscopy. Biochim Biophys Acta 1988;964:28–35.

[28] Davies MJ. Detection of peroxyl and alkoxyl radicals produced by reaction of hydroperoxides with rat liver microsomal fractions. Biochem J 1989;257:603–6.